

PRF Sampling Strategies for SwarmSAR Systems

Iannini, Lorenzo; Mancinelli, Alessandro; Lopez Dekker, Paco; Hoogeboom, Peter; Li, Yuanhao; Uysal, Faruk; Yarovoy, Alexander

DOI

[10.1109/IGARSS.2019.8898476](https://doi.org/10.1109/IGARSS.2019.8898476)

Publication date

2019

Document Version

Accepted author manuscript

Published in

IEEE International Geoscience and Remote Sensing Symposium (IGARSS)

Citation (APA)

Iannini, L., Mancinelli, A., Lopez Dekker, P., Hoogeboom, P., Li, Y., Uysal, F., & Yarovoy, A. (2019). PRF Sampling Strategies for SwarmSAR Systems. In *IEEE International Geoscience and Remote Sensing Symposium (IGARSS)* (pp. 8621-8624). Article 8898476 IEEE.
<https://doi.org/10.1109/IGARSS.2019.8898476>

Important note

To cite this publication, please use the final published version (if applicable).
Please check the document version above.

Copyright

Other than for strictly personal use, it is not permitted to download, forward or distribute the text or part of it, without the consent of the author(s) and/or copyright holder(s), unless the work is under an open content license such as Creative Commons.

Takedown policy

Please contact us and provide details if you believe this document breaches copyrights.
We will remove access to the work immediately and investigate your claim.

PRF SAMPLING STRATEGIES FOR SWARMSAR SYSTEMS

L. Iannini, A. Mancinelli, P. Lopez-Dekker, P. Hoogeboom, Y. Li, F. Uysal, A. Yarovoy

Delft University of Technology

ABSTRACT

The work investigates staggered and randomic PRF strategies for a close formation of small SAR satellites operating in a multistatic configuration. The satellites are positioned within a fraction of the along-track critical baseline, hence allowing for the application of Displaced Phase Center image formation approaches. The performance of regular and randomic pulse sampling schemes is in particular assessed for an MISO S-Band constellation, whose feasibility is further analyzed in relation to the number of satellites and their antenna size.

Index Terms— SAR system design, Multi-static geometry, pulse repetition frequency, staggered PRF, S-Band.

1. INTRODUCTION

The concept of Displaced Phase Center (DPC) antenna processing is not novel to the spaceborne radar community. Such spatio-temporal processing solution can either be used to identify ground moving targets (GMTI) or to augment the spatial resolution and the swath width of the system. The technique leverages on the use of multiple antennas, that can either be provided by independent subapertures of the same physical antenna or by multiple platforms, such as in the satellite configuration herewith debated. In the GMTI application scenario the choice of the pulse repetition frequency is not stringent, as the multiple channels can be coregistered by means of post-processing/interpolation. Conversely, in the case of its application for high-resolution enhancements, a perfect pulse interleave scenario shall be sought. In the simple case of $N = 2$ antennas, a half PRI offset should be ideally accounted between the antenna phase centers to attain a uniformly sampled signal with double PRF, as well as the most optimal ambiguity rejection conditions. For instance, in the case of a canonical system with a single physical antenna splitted in 2 subapertures, the PRI (or more precisely, its spatial equivalent) shall be set to one half of the antenna length. Such DPC condition is however more challenging to achieve with antennas hosted by different satellites, mainly because of the uncertainty on the along-track baselines. A multi-satellite formation demands therefore to handle irregularly sampled pulses, that must undergo an additional signal reconstruction phase.

Non-uniform sampling in spaceborne SAR has been

mainly debated for the two following staggered PRF scenarios: (a) multi-channel configurations, with channels characterized by the same constant PRF and with arbitrary phase center positions, not necessarily perfectly interleaved; (b) single-channel [1] and multi-channel [2] systems where the PRI is continuously varied, although with periodic patterns. The first scenario demands to merge N uniform grids with irregular offsets, and has been already covered by a few notable contributors [3][4]. A reconstruction strategy based on signal inversion in the frequency domain has been for instance suggested in [3]. An undesirable system singularity occurs when one or more offsets are equal to multiples of the PRI and hence no resolution enhancement can be obtained. The second staggered configuration is the one embraced by next generation DBF-capable systems [5][6] because of its capability of drifting the blind ranges along the aperture and hence to illuminate large swaths with a single pulse. In the context of this paper, however, the PRF continuous variation is itself the feature of interest because of its intrinsic performance invariance (in a statistical sense) to the phase center displacements. As illustrated in Fig. 1, the work here presented is indeed aimed at constellations of N satellites flying in close formation and operating in a MISO (Multiple Rx - Single Tx) configuration, where 1 monostatic and $N - 1$ bistatic stripmap images are produced. The study overlooks for the moment the synchronization and cross-track baseline challenges to focus on the azimuth sampling aspects. Two PRF strategies are in particular introduced and analyzed: a constant PRF strategy (associable to scenario (a)) where the performance is assessed as a function of the uncertainty on the along-track baselines; a continuously varying PRI strategy with completely randomic pattern.

2. METHODOLOGY

Let consider a swarm of N satellites flying on the same orbit with velocity v_s and along-track baselines $b_{ij} = |x_j - x_i| \ll B_c^{AT}$, hence where the distance between the 2 azimuth positions x_i and x_j is much shorter than the critical baseline B_c^{AT} , this latter depending on the antenna size L_a , assumed identical for all satellites. On a hypothetical MIMO scenario, the signal received by the ij channel can be related with a good approximation to the signal received by a different channel pq through

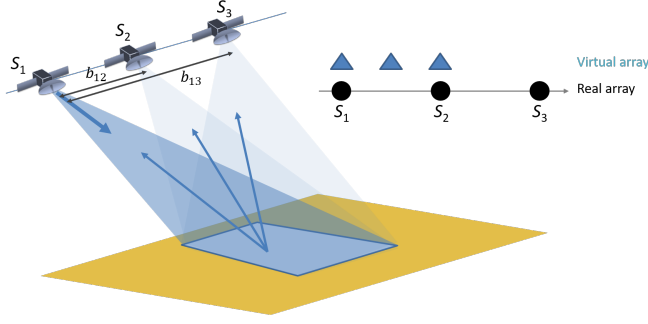


Fig. 1. Representation of the MISO SwarmSAR configuration for $N = 3$ satellites. The phase center location (virtual array) of the 3 channels is schematically reported on the right.

$$u_{ij}(t) \cong u_{kl} \left(t - \frac{\Delta b}{2v_s} \right) \exp \left(-\pi \frac{\Delta b^2}{\lambda v_s \rho_{kl}(t)} \right) \quad (1)$$

where $\Delta b = (x_p + x_q) - (x_i + x_j)$ is the equivalent monostatic baseline between the two acquisitions and the last term accounts for the difference physical baselines and hence the different 2-way distances ρ from the target (valid only for small baselines). In the case of the MISO configuration of Fig. 1, where only the first satellite is transmitting, and further compensating the signals for the baseline differences, equation (1) can be re-written as

$$u_i(t) \cong u_1 \left(t - \frac{b_i}{2v_s} \right) \quad (2)$$

where $u_i = u_{i1}$, $b_i \equiv b_{i1}$ and y_1 is the monostatic signal. The active satellite transmits pulses at azimuth times

$$t_n = \sum_{k=1}^n PRI(k) + t_0, \quad n \geq 1 \quad (3)$$

where the initial time t_0 is the first pulse of the considered synthetic aperture. A few configurations of the function $PRI(k)$ are now investigated.

2.1. Constant PRF

In such configuration the pulse interval is a constant value $PRI(k) \equiv 1/PRF$. The frequency domain representation of (2) takes the form

$$U_i(f) = U_1(f) \exp \left(-\pi f \frac{b_i}{v_s} \right) \quad (4)$$

with $u(t) \xrightarrow{\mathcal{F}} U(f)$. Since the signal is not continuous but it shall be instead addressed as discrete with PRI sampling interval, the observed spectrums become

$$Y(f) = \sum_{k=-\infty}^{+\infty} U(f - k \cdot PRF) \quad (5)$$

where each folding k represents a ghost of the scene, shifted in the image by an azimuth offset [7]

$$\tau = \frac{PRF}{f_R} k \quad \text{with} \quad f_R = \frac{2v_s^2}{\lambda r_0} \quad (6)$$

function of the doppler rate f_R and hence on the target zero-doppler distance r_0 .

In the case $N = 2$, by deriving the reconstructed signal expression through matched filter approach, i.e. unraveling the terms in $S(f) = Y_1(f)Y_1^*(f) + Y_2(f)Y_2^*(f)$, the power of the first ghost can be analytically approximated with

$$S_{amb}(k=1) \propto \cos \left(+\pi PRF \frac{b_2}{2v_s} \right). \quad (7)$$

The cosine argument confirms that a perfect rejection is achieved for interleaved pulses. Besides, the notch behaviour suggests that small errors in the PRF selection lead to significant degradation in the ambiguity performance. The same analytical method can be extended to a generic N -satellite case, yielding for the k -th ambiguity

$$S_{amb}(k) \propto \left| \sum_{n=1}^N \exp \left(-j\pi k PRF \frac{b_n}{v_s} \right) \right| \quad (8)$$

with $b_1 = 0$. When the baselines are known, the intensity of the first K ambiguities can hence be obtained by the sub-optimal estimate

$$P\hat{R}F = \underset{PRF}{\operatorname{argmin}} \sum_{k=1}^K \left| \sum_{n=1}^N \exp \left(-j\pi k PRF \frac{b_n}{v_s} \right) \right|^2 \quad (9)$$

that can be found through exhaustive search since the domain is monodimensional.

2.2. Randomic PRF

In this configuration, the pulse repetition interval is not defined by a function, but rather by a random process with uniform distribution

$$PRI \sim \mathcal{U}(PRI_{min}, PRI_{max}) \quad (10)$$

where the lower boundary on the PRI is given by the antenna size in elevation, L_e . Note that the technological implementation of completely randomic patterns is here neglected in order to focus on the theoretical concept comparison. Analogously to the patterned PRI scenarios discussed in [1], a random PRI system does not generate ambiguities that appear

as clear shifted replicas of the image, but rather it defocuses the ambiguities, spreading them on a larger area, or, for high $\Delta PRI = PRI_{max} - PRI_{min}$, on the whole scene. A notable advantage of a fully random PRI strategy is the invariance of the performance on the azimuth target position. Differently from the uniform PRF configuration, the choice of the two parameters, $PRI_{mean} = (PRI_{min} + PRI_{max})/2$ and ΔPRI , is not dependent on the baselines and hence can be done once for the whole mission.

2.3. Signal reconstruction

The signal reconstruction can be performed either in the frequency or in the time domain. The latter approach, proposed in [1], has been herewith adopted. The samples from the different channels must be then weighted and interpolated to a regular and more dense grid. This is done in through the Best Linear Unbiased (BLU) estimation that applies in practice a Kriging interpolation based on the PSD of the system. After the interpolation procedure, the interpolated signal is then compressed via the matched filter approach. If a uniformly illuminated antenna aperture is used in transmission as well as in reception, the azimuth PSD of $u(t)$ is given by

$$P_u(f) = \text{sinc}^4\left(\frac{L_a}{2v_s}f\right) \quad (11)$$

The normalized auto-correlation function $R_u(t)$ of the complex random process $u(t)$ is proportional to the inverse transform of $P_u(f)$ and takes the closed form

$$R_u(t) = \begin{cases} 0 & t \leq -\frac{2}{a} \\ \frac{a^3 t^3}{4} + \frac{3a^2 t^2}{2} + 3at + 2 & t \in]-\frac{2}{a}, -\frac{1}{a}] \\ -\frac{3a^3 t^3}{4} - \frac{3a^2 t^2}{2} + 1 & t \in]-\frac{1}{a}, 0] \\ \frac{3a^3 t^3}{4} - \frac{3a^2 t^2}{2} + 1 & t \in]0, \frac{1}{a}] \\ -\frac{a^3 t^3}{4} + \frac{3a^2 t^2}{2} - 3at + 2 & t \in]\frac{1}{a}, \frac{2}{a}] \\ 0 & t > \frac{2}{a} \end{cases} \quad (12)$$

where $a = \frac{2v_s}{L_a}$. The samples are hence assumed uncorrelated for $|t| > \frac{L_a}{v_s}$.

3. RESULTS AND DISCUSSION

A constellation of small satellites operating in S-Band is discussed. The relevant system concept specifications are reported in Table 1. Notice that two different azimuth antenna lengths are tested: 1 m for system A and 1.5 m length for system B. The antenna size in elevation is fixed to 1.5 m. Notice that such configuration leads to a swath width of 20 km in slant range and 30 km in ground range. Notice that the maximum allowed PRF in order to accommodate the swath, accounting for a duty cycle of 0.2, amounts to 4600 Hz approximately. In an ideally interleaved DPC system, three satellites

Table 1. Relevant specifications of the SwarmSAR system concept

Parameter	System A	System B
Frequency	3.2 GHz	
Orbit height	514 km	
Along-track baselines	200 m	
Antenna type	Planar array	
Antenna size, azimuth	1 m	1.5 m
Antenna size, elevation	1.5 m	
Antenna tilt, elevation	26	
Incidence angle near	26.3	
Incidence angle far	30.2	
Slant range near	568 km	
Skant range far	588 km	

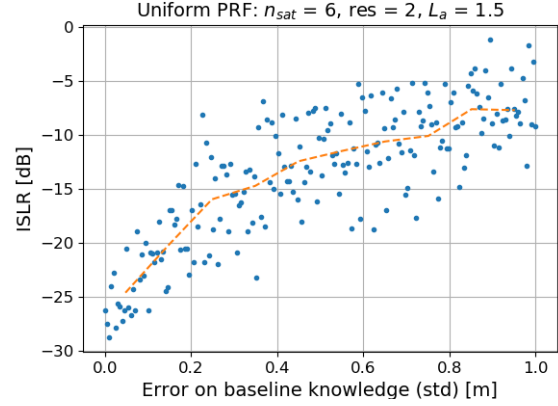


Fig. 2. Performance of a swarm system with uniform PRF = 4030 Hz for different uncertainties in the satellite AT baseline position.

would hence be sufficient to achieve an optimal ambiguity rejection. Two consecutive satellites are separated by an average (along-track) baseline of 200 m. In practice, a random component is introduced on their position for a statistical performance assessment over 20 baseline realizations.

The analysis will focus on the azimuth ambiguity performance. In order to compare the uniform and random PRF strategies the Integrated Side-Lobe Ratio (ISLR) metric will be adopted. The canonical azimuth ambiguities to signal ratio expressions are in fact not suited for continuously varying PRI systems. Note that a Hann window has applied during the focusing process in order to improve the ISLR performance. Consequently, a decrease in the resolution by a factor 2 has to be accounted on the top of the processed bandwidth. In the random sampling scenario, a PRF range of 20 Hz between 4010 and 4030 Hz is selected, as shown in the timing diagram in 3. The performance of the random PRF scenario is compared to the one with uniform PRF = 4020 Hz. The latter is however dependent on the application of (9) and hence

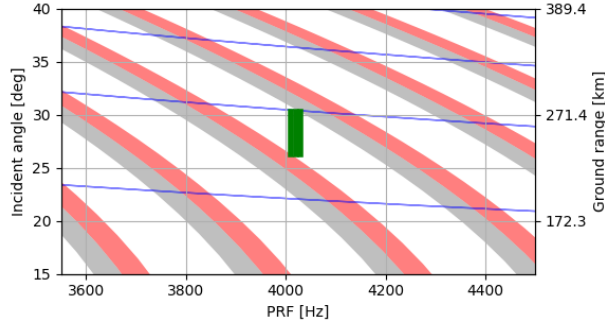


Fig. 3. Timing diagram of a random PRF system. The chosen 20 Hz range is reported in green.

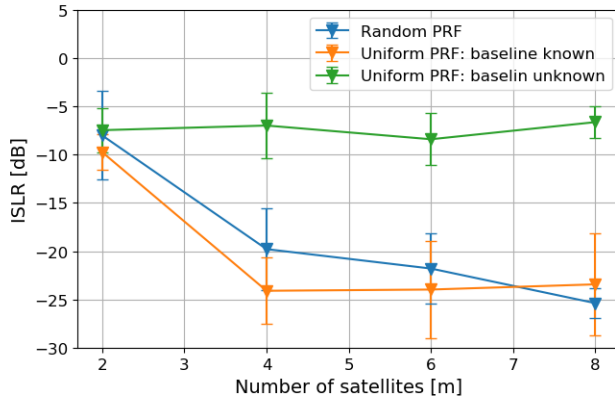


Fig. 4. Performance for antenna length $L_a = 1.5$ m as a function of the number of satellites in the swarm.

on the uncertainties on the satellite position. It is shown in Fig. 2 that a standard deviation of 20 cm can raise the ISLR to -15 dB with 6 satellites. Such degradation would be more significant for a lower number of satellites N . Notice as well that the performance must be always addressed in a statistical sense. The two extreme cases for the uniform PRF system, i.e. that of perfect baseline knowledge and that of no knowledge at all, are adopted in Fig. 4 for the comparison with the random PRF system. Notice that the random sampling strategy comes close to the best uniform sampling for $N > 4$. Even a low PRF bandwidth of 20 Hz is hence sufficient to prevent the occurrence of gaps along the all orbit due to unfortunate along-track positioning. Furthermore, a random PRF strategy would have the notable advantage of being performance-independent from the baseline information and hence on the technological solutions demanded to update it before the acquisition.

Acknowledgment

The work has been carried out within the framework of the NL-RIA project funded by the Netherlands Organisation for Scientific Research (NWO).

4. REFERENCES

- [1] M. Villano, G. Krieger, and A. Moreira, "Staggered SAR: High-Resolution Wide-Swath Imaging by Continuous PRI Variation," *IEEE Transactions on Geoscience and Remote Sensing*, vol. 52, no. 7, pp. 4462–4479, July 2014.
- [2] F. Queiroz de Almeida, M. Younis, G. Krieger, and A. Moreira, "Multichannel Staggered SAR Azimuth Processing," *IEEE Transactions on Geoscience and Remote Sensing*, vol. 56, no. 5, pp. 2772–2788, May 2018.
- [3] G. Krieger, N. Gebert, and A. Moreira, "Unambiguous SAR signal reconstruction from nonuniform displaced phase center sampling," *IEEE Geoscience and Remote Sensing Letters*, vol. 1, no. 4, pp. 260–264, Oct. 2004.
- [4] I. Sikaneta, C. H. Gierull, and D. Cerutti-Maori, "Optimum Signal Processing for Multichannel SAR: With Application to High-Resolution Wide-Swath Imaging," *IEEE Transactions on Geoscience and Remote Sensing*, vol. 52, no. 10, pp. 6095–6109, Oct. 2014.
- [5] P. Rosen, S. Hensley, S. Shaffer, W. Edelstein, Y. Kim, R. Kumar, T. Misra, R. Bhan, and R. Sagi, "The NASA-ISRO SAR (NISAR) mission dual-band radar instrument preliminary design," in *2017 IEEE International Geoscience and Remote Sensing Symposium (IGARSS)*, July 2017, pp. 3832–3835.
- [6] A. Moreira, G. Krieger, I. Hajnsek, K. Papathanassiou, M. Younis, P. Lopez-Dekker, S. Huber, M. Villano, M. Pardini, M. Eineder, F. De Zan, and A. Parizzi, "Tandem-L: A Highly Innovative Bistatic SAR Mission for Global Observation of Dynamic Processes on the Earth's Surface," *IEEE Geoscience and Remote Sensing Magazine*, vol. 3, no. 2, pp. 8–23, June 2015.
- [7] A. M. Guarnieri, "Adaptive removal of azimuth ambiguities in SAR images," *IEEE Transactions on Geoscience and Remote Sensing*, vol. 43, no. 3, pp. 625–633, Mar. 2005.